Chinese Chemical Letters xxx (2016) xxx–xxx

Contents lists available at ScienceDirect

Chinese Chemical Letters

journal homepage: www.elsevier.com/locate/cclet

Review

Graphene-based materials for polymer solar cells

Xiao-Feng Lin [a,b,1], Zi-Yan Zhang [a,b,1], Zhong-Ke Yuan [a,b], Jing Li [a,b], Xiao-Fen Xiao [a,b], Wei Hong [a,b], Xu-Dong Chen [a,b,*], Ding-Shan Yu [a,b,*]

[a] Key Laboratory for Polymeric Composite and Functional Materials of Ministry of Education of China, School of Chemistry and Chemical Engineering, Sun Yat-sen University, Guangzhou 510275, China
[b] Key Laboratory of High Performance Polymer-based Composites of Guangdong Province, School of Chemistry and Chemical Engineering, Sun Yat-sen University, Guangzhou 510275, China

ARTICLE INFO

Article history:
Received 3 May 2016
Received in revised form 8 June 2016
Accepted 21 June 2016
Available online xxx

Keywords:
Graphene
Polymer solar cells
Electrodes
Interfacial layers
Active layers

ABSTRACT

Due to the remarkable electronic, optical, thermal, and mechanical properties, graphene-based materials have shown great potential in a wide range of technique applications. Particularly, the high transparency, conductivity, flexibility, and abundance make graphene materials highly attractive for polymer solar cells (PSCs). Graphene-based materials have been regarded as one promising candidate used in various parts in PSCs not only as electrodes, but also as interfacial layers and active layers with an aim to boost the power conversion efficiency of the devices. In this review, we summarize the recent progress about the design and synthesis of graphene-based materials for efficient PSCs along with the related challenges and future perspectives.

1. Introduction

During the past decades, polymer solar cells (PSCs) have attracted tremendous interest due to a variety of competitive advantages, such as flexibility, lightweight, low-cost processing and suitability for industrial manufacturing of large-area and flexible devices [1–5]. With the development of novel photovoltaic materials [6–9], the improvement of fabrication processing [10] and optimization of device structures [11,12], a 10% of the power conversion efficiency (PCE) have broken through for PSCs with either single junction [13] or tandem structure [14]. However, in comparison with the conventional and commercial photovoltaic devices, such as silicon solar cells, further improvements of the PCE and long-term stability of PSCs are still highly required. Besides, it is known that the overall device performance for these solar cells strongly depends not only on the device structure, but also on the properties of the materials. Therefore, developing new materials, which can be used as the different parts of solar cells such as the electrodes, active layers and interfacial layers, as well as the related device fabrication techniques, is of great significance.

Graphene, a novel two-dimensional (2D) carbon material with single-atomic-thick and sp^2-bonded, has attracted tremendous attention in a wide range of research areas [15–18]. Due to the remarkable electronic, optical, thermal, and mechanical properties [4], graphene-based materials have been widely used for emerging energy conversion and storage systems such as supercapacitors, fuel cells, batteries and solar cells [19–23]. Particularly, the high transparency, conductivity, flexibility, and abundance make graphene materials highly attractive for PSCs. Theoretical PCEs as high as 12% have been predicted for graphene-based organic devices [24], and it has also been proposed that graphene may favor charge carrier multiplication [24]. As for practical device applications, graphene has proved to be useful in various parts of PSCs with extraordinary performance, not only as a substitute for indium tin oxide (ITO) electrodes, but also as cathode, electron acceptor, hole extraction and electron extraction material [25–30]. In this review, we summarize the research progress about graphene-based PSCs, in which graphene-based materials were used in different layers of PSCs including electrodes, interfacial layers and active layers. Meanwhile, the challenges and the future development of graphene-based materials for highly efficient PSCs is also discussed.

* Corresponding authors at: Key Laboratory for Polymeric Composite and Functional Materials of Ministry of Education of China, Key Laboratory of High Performance Polymer-based Composites of Guangdong Province, School of Chemistry and Chemical Engineering, Sun Yat-sen University, Guangzhou 510275, China.
E-mail addresses: cescxd@mail.sysu.edu.cn (X.-D. Chen), yudings@mail.sysu.edu.cn (D.-S. Yu).
[1] These authors contributed equally to this work.

http://dx.doi.org/10.1016/j.cclet.2016.06.041
1001-8417/

2. Graphene-based materials as electrodes

Due to high conductivity and transparency, the most important application of graphene is for transparent conductive electrodes of PSCs. It is well known that transparent conductive electrodes are essential components of PSCs. Traditionally, ITO plays a key role as transparent conductive electrodes for PSCs, but it has some disadvantages including high cost due to the limited indium source, susceptibility to ion diffusion into polymer layers, fragility, instability in acid or base, and poor transparency in near infrared region [17,31]. Thus, a substitute for ITO with similar performance but lower cost is highly required. In this regard, graphene has been regarded as a promising transparent electrode material due to the high transparency, excellent conductivity, highly flexible nature, and elemental abundance [32–39].

Graphene-based materials including chemically or thermally reduced graphene oxide (rGO) derived from graphene oxide (GO) and graphene grown by chemical-vapor-deposition (CVD) have been exploited as transparent conductive electrodes to replace conventional ITO electrodes in PSCs. Yin *et al.* [32] used an rGO film on a polyethylene glycol terephthalate (PET) substrate as the transparent conductive electrode, producing highly flexible PSCs. The rGO film was fabricated by the thermal annealing of a spinning-coated GO film under the H_2/Ar atmosphere at 1100 °C for 2 h. Such top-down approach is more favorable than a bottom-up approach such as CVD from the viewpoint of mass production potential. A higher PCE of 0.78% was achieved when using rGO films with a thickness of 16 nm, sheet resistance of 3.2 kΩ/square and transmittance of 65% (Fig. 1). Notably, the obtained device with an rGO film on the PET electrode can withstand up to 1200 bending cycles without compromising the overall device performance (Fig. 1A), while traditional ITO-based devices with the identical device configuration easily crack upon bending together with the degradation of the device performance associated with the brittle nature of ITO. This work opens up an avenue to develop flexible optoelectronic devices using graphene-based transparent electrodes.

Similarly, Chen *et al.* [33] employed another kind of rGO film, produced through hydrazine vapor exposure and subsequent thermal annealing in insert conditions, as a transparent electrode for poly (3-hexylthiophene) (P3HT) and phenyl-C61-butyric acid methyl ester (PCBM)-based bulk heterojunction solar cells (Fig. 2). It was found that both transparency and conductivity of the rGO electrodes are dependent on the thickness of the rGO film. The optimized device using the rGO electrode obtained a PCE of 0.13%, while the standard ITO-based device with the same configuration has a PCE of 3.59%. The unsatisfactory PCE, most probably, comes from higher sheet resistance of the rGO film as well as its poor compatibility with the poly (3,4-ethylenedioxythiophene):poly (styrene sulfonic acid) (PEDOT:PSS) layer associated with the hydrophobic surface of rGO. Although the PCE for the device based on rGO electrodes is still inferior to that of the standard ITO-based device, this work provides a low-cost and simple solution process for producing conductive and transparent graphene films to replace traditional ITO electrodes, which makes such graphene-based window electrodes versatile for a range of optoelectronic applications, not limiting to PSCs. Meanwhile, it is highly anticipated that the performance of these graphene-electrode-based solar cells should be enhanced significantly by optimizing the conductivity of graphene electrodes and surface wetting property of graphene films.

Recently, inspired by the widely-used metal-grid electrodes with high transparency, Chen *et al.* [34] invented a new kind of graphene mesh electrodes (GMEs), which were fabricated by the standard industrial photolithography and O_2 plasma etching process using graphene solution (Fig. 3A). Using the standard photolithography technique, such graphene mesh electrode patterns can be controlled precisely to achieve a balance of conductivity and transparency. When using such GMEs with a sheet resistance of 608 Ω/square and transmittance of 55% as the transparent electrode, and P3HT:PCBM as the active layer, the fabricated PSCs exhibited a PCE of up to 2.04%, which is comparable to that of ITO-based devices (3.00%) (Fig. 3B). The device performance is expected to be improved by optimizing the transparency of the GMEs and controlling the interfacial contact between the graphene electrode and the PEDOT:PSS layer. Considering that the standard photolithography technique is a conventional technology in the semiconductor industry, this work provides a new path for producing graphene mesh transparent electrodes on a large scale for optoelectronic devices.

Apart from chemically or thermally rGO, the CVD-grown graphene has also been widely investigated as transparent electrodes to replace ITO electrodes for PSCs. Choi *et al.* [35] fabricated the PSCs using CVD-grown multilayer graphene (MLG) on glass substrates as transparent electrodes (see Fig. 4). The MLG electrode showed high transparency up to 84.2% and lower sheet resistance (374 ± 3 Ω/square). The bulk heterojunction PSCs with the MLG transparent electrode and the P3HT:PCBM active layer exhibited a PCE of 1.17%. Such PCE value was better than those of the devices using chemically rGO electrodes by the top-down approach. This is mainly because the graphene electrode by CVD can render higher conductivity relative to chemically rGO electrodes.

Followed by the above work, Liu *et al.* [36] used single-layer graphene film by the CVD method as the top electrode and the ITO as the bottom electrode to fabricate a semitransparent solar cell based on P3HT:PCBM. The conductance of the graphene electrode

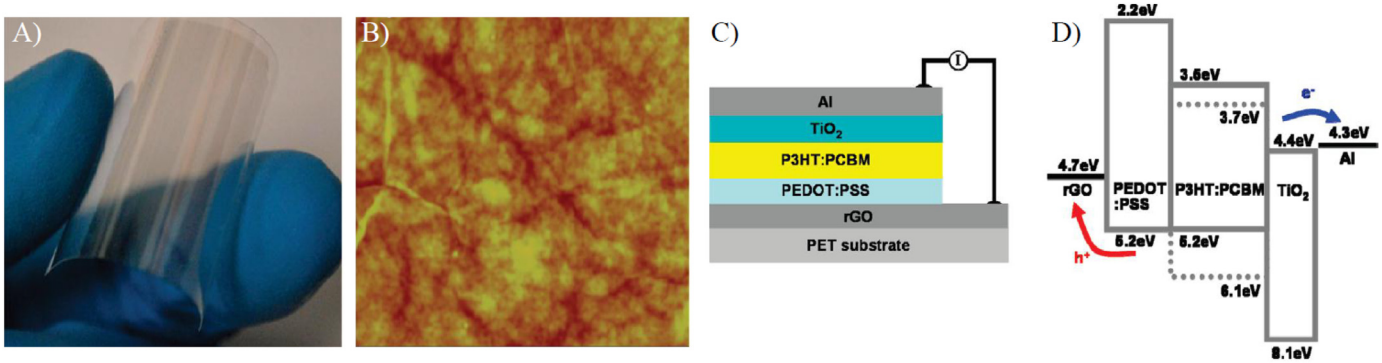

Fig. 1. (A) Photographic of rGO on the PET substrates; (B) atomic force microscope (AFM) image of rGO/PET; schematic representation of (C) the layer structure and (D) energy level for the PSCs, *i.e.*, rGO/PEDOT:PSS/P3HT:PCBM/TiO_2/Al, with rGO as the transparent electrode. Reproduced with permission from Ref. [32].

Please cite this article in press as: X.-F. Lin, et al., Graphene-based materials for polymer solar cells, Chin. Chem. Lett. (2016), http://dx.doi.org/10.1016/j.cclet.2016.06.041

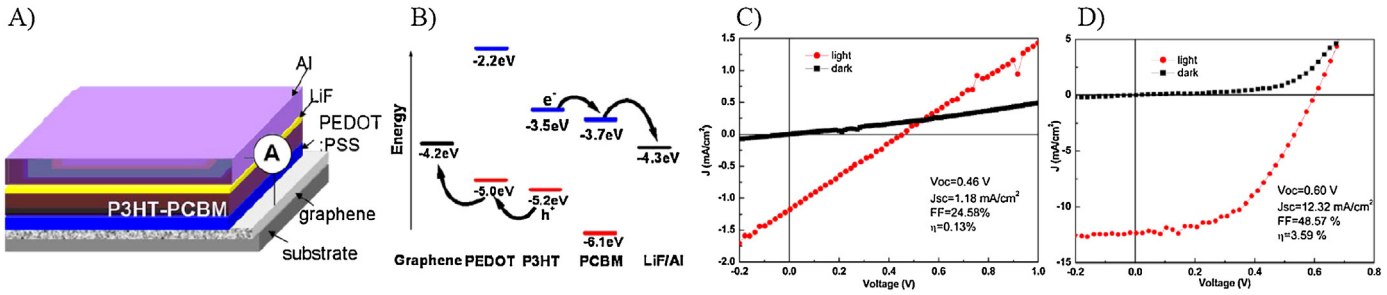

Fig. 2. (A, B) Device structure and energy diagram of the fabricated device with structure Graphene/PEDOT:PSS/P3HT:PCBM/LiF/Al. (C) Current density–voltage (*J*–*V*) curves of P3HT:PCBM bulk heterojunction solar cells with 25 nm thick graphene films as the transparent anode. (D) Current density–voltage (*J*–*V*) curves of P3HT:PCBM bulk heterojunction PSCs with ITO as anode. Reproduced with permission from Ref. [33].

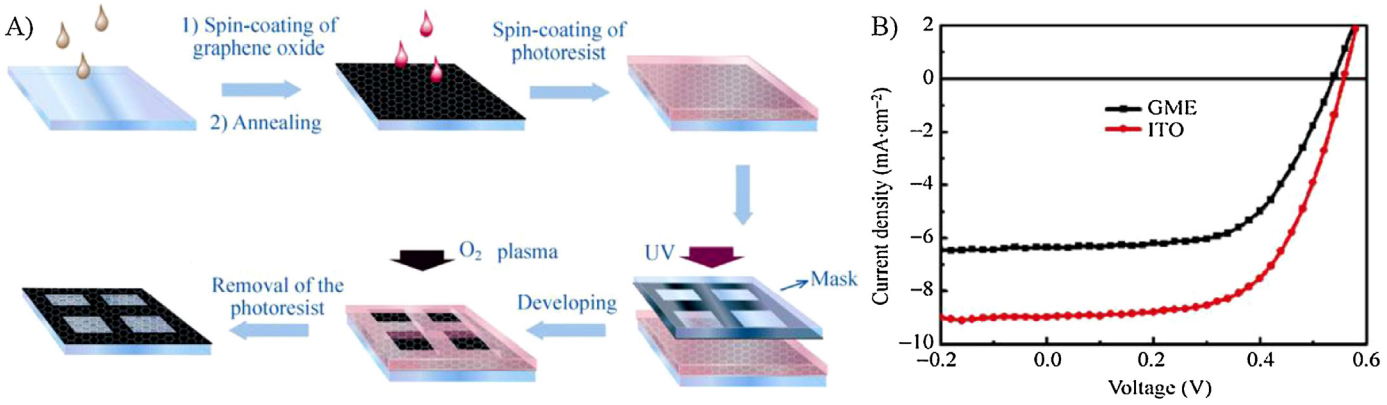

Fig. 3. (A) Illustration of the schematic steps for the preparation of the graphene mesh electrodes. (B) *J*–*V* curves of the anode/PEDOT:PSS/P3HT:PCBM/LiF/Al PSCs with ITO (red) or GME (black) as the anode under illumination of AM.1.5, 100 mW/cm^2. Reproduced with permission from Ref. [34].

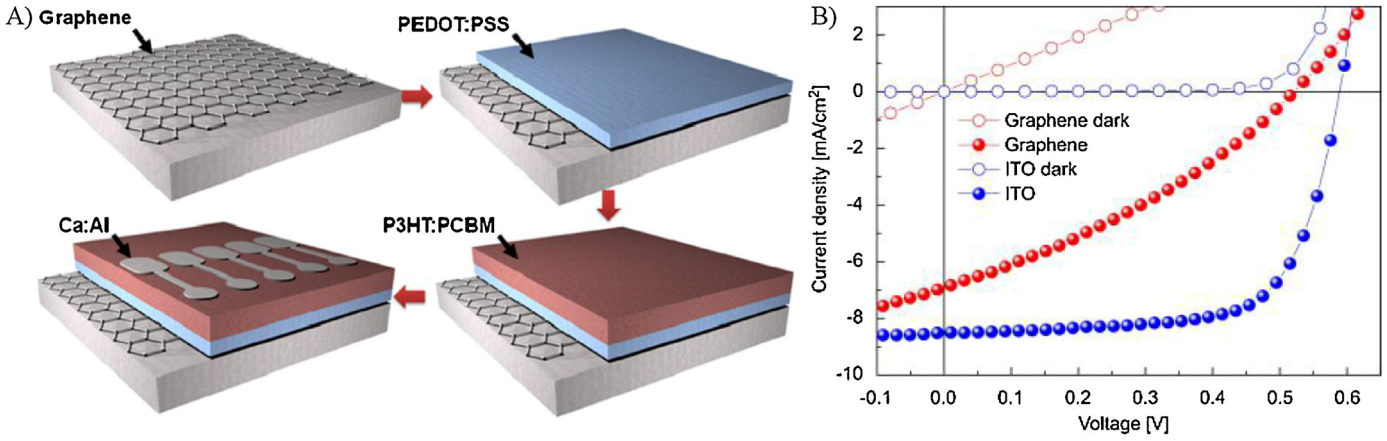

Fig. 4. (A) Schematics of bulk-heterojunction PSCs on a MLG electrode showing MLG anode and Al:Ca cathode patterns. (B) *J*–*V* curves (AM 1.5 G with an incident light power intensity of 100 mW/cm^2) of PSCs fabricated on the MLG electrode and reference ITO electrodes. Reproduced with permission from Ref. [35].

can be enhanced by doping the graphene film with Au nanoparticles and PEDOT:PSS (Fig. 5A), which led to an increase of conductance for more than 400%. The overall performance of the solar cell can be optimized by using the doped graphene electrode and the maximum efficiency up to 2.7% was achieved. Interestingly, the semitransparent PSCs showed higher efficiency illuminated from graphene than from the ITO side (Fig. 5B), which was attributed to the better transmittance of the graphene electrodes. It is expected that PSCs with higher efficiency can be achieved by using single-layer graphene with better quality and more optimized processing conditions.

Recently, Liu *et al.* [37] used highly doped multilayer CVD graphene as top transparent electrodes and P3HT:PCBM as active layers to fabricate another package-free flexible polymer solar cell on polyimide (PI) substrates. As shown in Fig. 6, this device structure is graphene/PEDOT:PSS/P3HT:PCBM/ZnO/Ag/PI. After doping with PEDOT:PSS and Au nanoparticles on the surface, the optimized PCE with the two-layer graphene as the top electrode was up to 3.2% (Fig. 6). Notably, its PCE decreased by only 8% after 1000 bending cycles, showing superior flexibility and stability. More interestingly, it was found that air cannot diffuse across the narrow space between two graphene layers, thus

Please cite this article in press as: X.-F. Lin, et al., Graphene-based materials for polymer solar cells, Chin. Chem. Lett. (2016), http://dx.doi.org/10.1016/j.cclet.2016.06.041

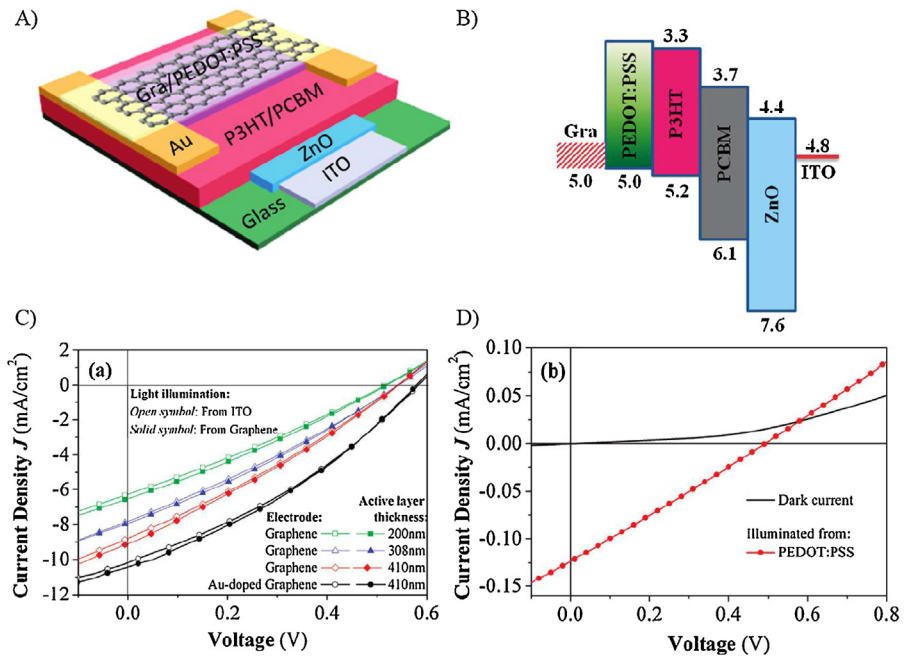

Fig. 5. (A) Schematic diagram of a semitransparent PSC with the structure Glass/ITO/Zinc Oxide(ZnO)/P3HT:PCBM/PEDOT:PSS/graphene and band structure of the PSCs. (B) *J–V* characteristics measured from two sides of semitransparent PSCs with graphene top electrodes and different active layer thicknesses. (C) *J–V* characteristics of a PSC with PEDOT:PSS top electrode. Reproduced with permission from Ref. [36].

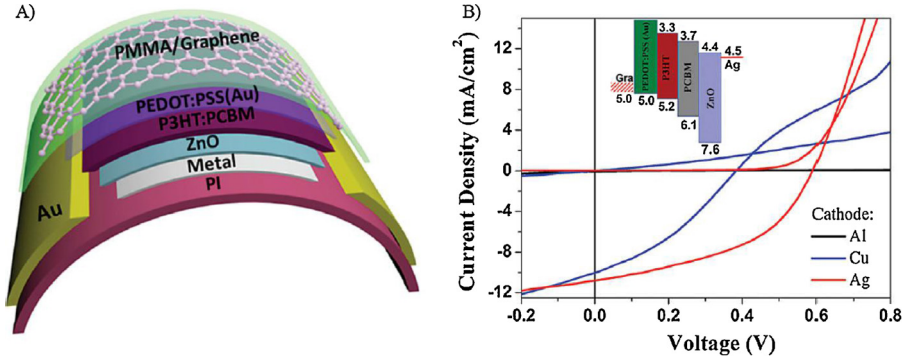

Fig. 6. (A) Schematic diagram of a PSC with the inverted structure: PI/Metal/ZnO/P3HT:PCBM/PEDOT:PSS(Au)/Graphene/PMMA. (B) *J–V* characteristics of PSCs with different metals as cathode and single-layer graphene as anode. Reproduced with permission from Ref. [37].

rendering excellent packaging effect on flexible solar cells. Thus, these flexible devices with graphene top electrodes may not require additional packaging, and can provide many advantages such as simplifying the device fabrication, enhancing the device flexibility and reducing the device cost. Continuing the above effort, Liu *et al.* [38] demonstrated the fabrication of another new semitransparent solar cell with graphene transparent electrodes as both cathode and anode. Such unique all-graphene electrodes can absorb light from both sides and the PCE is up to 3.4%. Considering that the devices are mainly made of carbon, the devices are environmental friendly and low-cost. This work paves a way for realizing high-performance carbon-based optoelectronic devices. Thus, these two results imply that graphene is an excellent candidate for the transparent electrodes of flexible solar cell as well as other organic devices especially air sensitive ones. Similarly, other promising results using a graphene-based transparent electrode have also been reported [39].

Clearly, graphene made either by top-down approaches starting from GO or bottom-up approaches like CVD has great potential as a transparent electrode to replace traditional ITO electrodes for PSCs. In particular, graphene-based transparent electrodes can be used as flexible electrodes for optoelectronic devices. It is noted that the two key parameters for the graphene transparent electrodes, conductivity and transparency, strongly depend on the preparation method. Chemically processing method demonstrates some advantages such as low cost, simplicity of preparation technique, and ease of scale-up for practical applications. However, there is an unavoidable tradeoff between transparency and conductivity for chemically processed rGO. Chemically processed rGO also suffers from some drawbacks including the contact resistance of the small graphene sheets and the relatively low conductivity associated with the structural defects from chemically reduced graphene sheets, thus limiting the device performance. In contrast, CVD grown graphene possesses much better conductivity and higher quality. But the CVD method usually involves high-temperature and multi-step processing and is not favorable for large-area processing. Thus, it is still huge challenge to seek new preparation methods to

Please cite this article in press as: X.-F. Lin, et al., Graphene-based materials for polymer solar cells, Chin. Chem. Lett. (2016), http://dx.doi.org/10.1016/j.cclet.2016.06.041

produce continuous and large–area graphene thin film with a good balance of high conductivity and high transparency.

3. Graphene-based materials as interfacial layers

The interfacial layers, such as the hole extraction layer (HEL) or electron extraction layer (EEL) between the active layer and the anode/or cathode respectively, play an important role in determining the overall device performance of PSCs [40]. In primitive PSCs, the active layers (donor and acceptor) are in direct electrical contact with the electrodes (cathode and anode), leading to the recombination of charge carriers and the leakage current. In order to minimize such adverse effects, the HEL and EEL are used as interfacial layers to align the energy levels between the work function of the anode and the highest occupied molecular orbital (HOMO) level of the electron donor, as well as the work function of the cathode and the lowest unoccupied molecular orbital (LUMO) level of electron acceptor, respectively. Conventionally, PEDOT:PSS has been commonly used as HEL in PSCs, but it has some drawbacks such as low transmittance in the red to near infrared (NIR) region, strong acidic and hygroscopic nature, which have a detrimental effect on PCE and stability of PSCs [41,42]. On the other hand, the low-work-function metals or their related salts, metal oxide semiconductors and conjugated polyelectrolyte have often been used as EELs [43,44]. As EELs, materials need to have a low work function for electrons to be efficiently transported to the cathode. During the past decades, graphene-based materials have been developed as interfacial layers in PSCs, owing to its extraordinary electrical conductivity, optical transparency and tunable optoelectronic properties [45–50]. GO and its derivatives have been demonstrated not only as the HEL in PSCs that presented attractive results relative to PEDOT:PSS, but also as the EEL for PSCs with high PCE, due to their advantages of less corrosion for the ITO electrode and a better energy-band structure for efficient charge transport.

For example, Li *et al.* [51] made a pioneer work, which used the GO thin film as HEL in PSCs in 2010. They fabricated a PSC with the device structure of ITO/GO/P3HT:PCBM/Al (Fig. 7A). The proposed GO-based HEL had the work function of 4.9 eV to match well with the LUMO level of the donor (P3HT) and the work function of ITO (Fig. 7B). The optimized PCE of the device using GO as the HEL was up to 3.5%, which is comparable to those of conventional PSCs using PEDOT:PSS as the HEL (3.6%) and much higher than those of the devices without the HEL (1.8%) (Fig. 7C). Furthermore, the device with GO as HEL demonstrated significantly improved long-term stability, possibly due to effective suppression of the leakage current and separation of the carriers. However, while the thickness of the GO layer increased from 2 nm to 10 nm, the PCE of the device dramatically decreased from 3.5% to 0.9% (Fig. 7D), due to the increased series resistance *via* increasing thickness arising from the insulate nature of GO. Therefore, the thicker GO film can produce the higher sheet resistance that will lead to a lower short circuit current (J_{sc}), fill factor (FF) and transparency for the PSCs. Despite the exciting results with GO as HEL mentioned above, the device performance still suffers from the insulate nature and thickness-dependent properties of GO.

To address the aforementioned issues associated with the insulated GO, reduction of GO into rGO is a good solution to improve the conductivity of GO as HEL in PSCs [52]. Kim *et al.* [53] demonstrated moderately-reduced GO films, by thermal annealing of solution-processed GO film at 150, 250, and 350 °C for 10 min in air, to replace conventional PEDOT:PSS as HELs in PSCs (Fig. 8). The optimized conductivity of rGO films can reach 1.8 S/m after the reduction by thermal annealing at 250 °C. The PCE of the PSCs with P3HT:PCBM as the active layer increased from 1.47% to 3.98%, which is comparable to that of the reference devices containing PEDOT:PSS HELs (3.85%). Moreover, the rGO-based PSCs with the thermal-annealing method exhibited superior device stability relative to the conventional PEDOT:PSS-based PSCs. Unfortunately, such approach is restricted to be used in the PSCs with glass substrates, while the plastic substrates in flexible PSCs usually cannot tolerate the high temperature (>200 °C) required for the thermal annealing of the prefabricated GO.

Considering that the work function of GO (only 4.6–4.9 eV) is much lower than the HOMO of the organic semiconductors (typically >5.1 eV) leading to interface barriers in terms of hole injection or extraction from the electrodes to the active layers, tuning the work function of GO is another research direction to achieve efficient graphene-based HEL. Dai *et al.* [54] designed a solution-processable sulfated GO (GO-OSO_3H), which can be utilized as a HEL in PSCs. They introduced the strongly acidic moiety (SO_3H) into the carbon basal plane of GO, as shown in Fig. 9A, which affording solution processability, enhancing the interfacial doping of the electron-donor, and improving the conductivity of the GO-OSO_3H due to the dehydration effect of the fuming sulfuric acid used as a reactant. What is more, the work function of sulfated GO slightly increased from 4.7 eV of GO to 4.8 eV, which matches the HOMO level of P3HT. As a result, PSC devices with GO-OSO_3H as the HEL showed excellent device performance with a high PCE of up to 4.37%. Moreover, the device performance was nearly independent of the GO-OSO_3H layer thickness (Fig. 9B), which was in stark contrast to the aforementioned device with the insulating GO as the HEL. Therefore, compared with other hole-extraction materials like PEDOT:PSS and metal oxides, graphene-based materials have shown great promise as HELs for highly efficient PSCs.

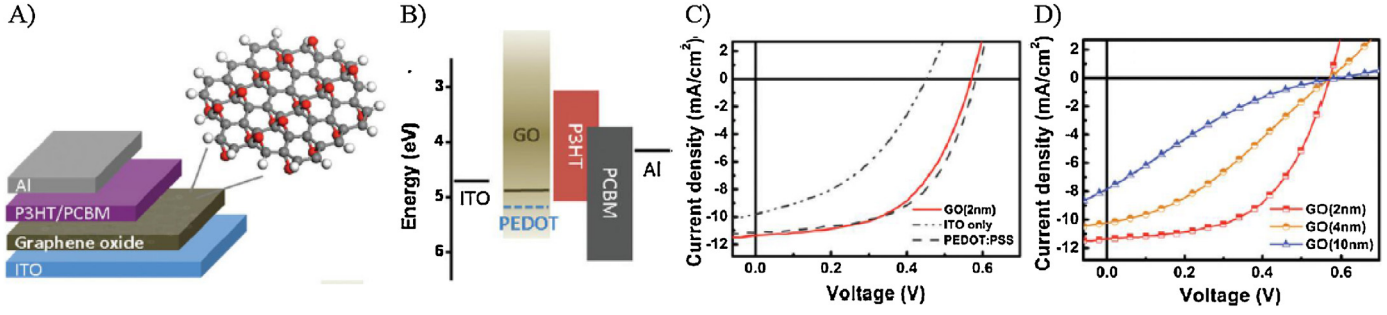

Fig. 7. (A) Schematic of the device structure consisting of the following: ITO/GO/P3HT:PCBM/Al. (B) Energy level diagrams of the bottom electrode ITO, interlayer materials (PEDOT:PSS, GO), P3HT (donor), and PCBM (acceptor), and the top electrode Al. (C) *J–V* characteristics of photovoltaic devices with no hole transport layer (curve labeled as ITO), with 30 nm PEDOT:PSS layer, and 2 nm thick GO film. (D) *J–V* characteristics of ITO/GO/P3HT:PCBM/Al devices with different GO thickness. All of the measurements were under simulated A.M. 1.5 illumination at 100 mW/cm^2. Reproduced with permission from Ref. [51].

Please cite this article in press as: X.-F. Lin, et al., Graphene-based materials for polymer solar cells, Chin. Chem. Lett. (2016), http://dx.doi.org/10.1016/j.cclet.2016.06.041

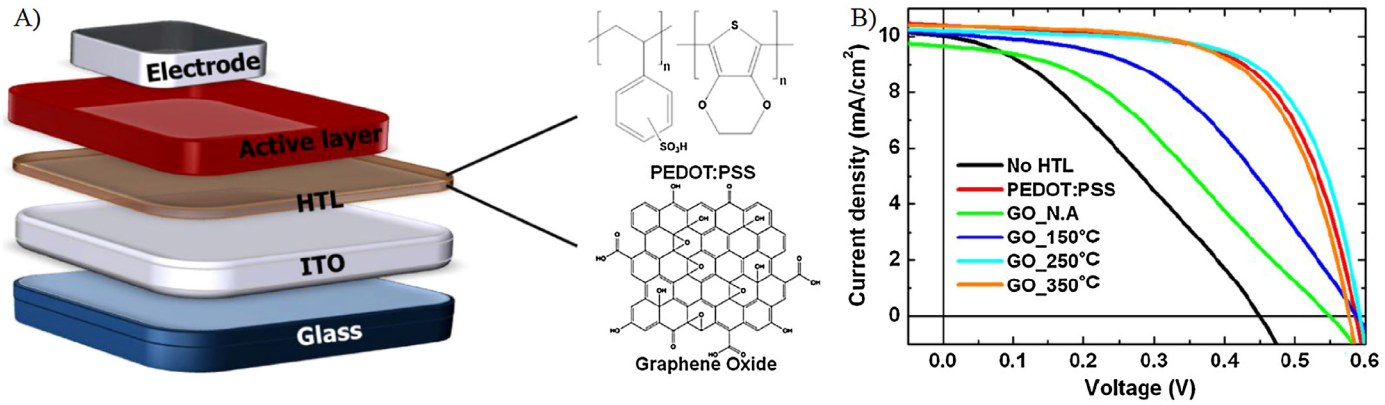

Fig. 8. (A) Schematic of PSCs fabricated with PEDOT:PSS and GO. (B) Representative *J–V* characteristics of devices prepared using thermally reduced GO. Reproduced with permission from Ref. [53].

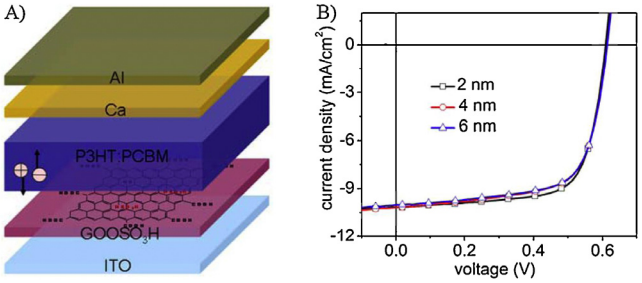

Fig. 9. (A) Schematic of the device structure. (B) *J–V* curves of the PSC devices with GO-OSO_3H with different thicknesses. Reproduced with permission from Ref. [54].

Alternatively, Li *et al.* [55] designed and synthesized chlorinated GO (Cl-GO) by using dichlorobenzene to react with GO thin film under UV irradiation. Chlorinated degree of Cl-GO can be controlled by adjusting the processing time of the UV irradiation, which can realize the continuous tuning of work function of Cl-GO film from 4.9 eV to 5.2 eV (Fig. 10B). The Cl-GO film on ITO has higher transparency relative to PEDOT:PSS, which allows the maximum photon flux to reach the active layer. The cells with Cl-GO film (5.2 eV) as HEL and poly[(4,8-bis-(2-ethylhexyloxy)-benzo[1,2-b;4,5-b′]dithiophene)-2,6-diyl-alt-(4-(2-ethylhexanoyl)-thieno[3,4-b]thiophene)-2,6-diyl](PBDTTT-C): (6,6)-phenyl-C-71-butyric acid methylester ($PC_{71}BM$) as the active layer achieved a PCE of up to 7.6%, much better than that of the conventional PEDOT:PSS device (6.53%, Fig. 10B, Table 1). This work moves one step closer to the practical application of graphene-based materials as an alternative to conventional PEDOT:PSS for optoelectronic devices.

Different from HELs with high work function, EEL materials should have a low work function, which can match the LUMO level of the acceptor materials to promote the electron extraction and result in the decrease of charge carrier recombination and series resistance. Due to tunable energy level of graphene-based materials by controlled functionalization, they can be used as amibipolar transporting materials for efficient extraction of both holes and electrons [56]. Therefore, n-type doped GO can be regarded as EELs in PSCs *via* simple spin-coating method, which is a promising candidate to replace the conventional EELs (*e.g.* Ca and LiF) prepared necessarily by thermal vacuum evaporation. Liu *et al.* [57] firstly reported cesium-neutralized GO (GO-Cs) (as shown in Fig. 11) as interfacial materials of cathodes in PSCs. By replacing the periphery –COOH with the –COOCs groups through charge neutralization, the work function of the GOCs can be reduced to 4.0 eV, matching well with the LUMO level of PCBM for efficient electron extraction. The cell based on GO-Cs exhibited a PCE of up to 3.08%, fairly comparable to that of the device using LiF (3.15%), showing the great capability of GO-Cs as the electron extraction material in solar cells.

In addition to 2D GO-based materials, graphene quantum dots (GQDs) have emerged as another promising candidate for HELs or EELs due to unique zero-dimensional (0D) structure and optoelectronic properties. In 2013, Yang *et al.* [58,59] have used Cs_2CO_3 functionalized GQDs (GQDs-Cs_2CO_3) as EEL for inverted PSCs. In comparison with inverted PSCs using Cs_2CO_3 as the EEL and P3HT:PCBM as the active layer, the device using GQDs-Cs_2CO_3 as the EEL exhibited 18.8% improvement in PCE from 2.72% to 3.23%, as well as 200% enhancement in stability. The PCE enhancement is

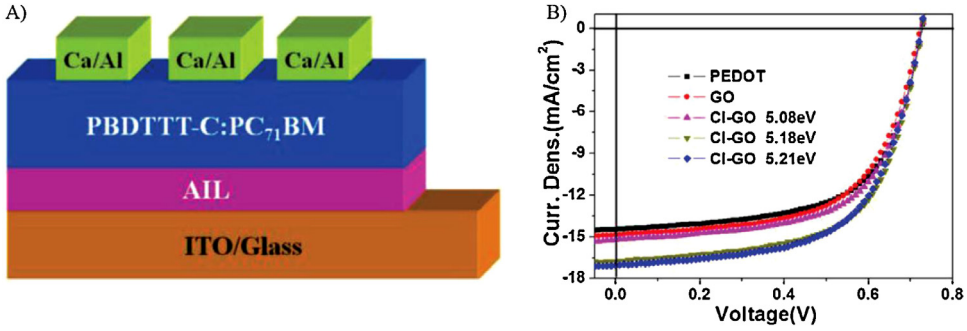

Fig. 10. (A) The structure of PSCs with Cl-GO as HELs. (B) *J–V* curves based on P3HT:PCBM with Cl-GO. Reproduced with permission from Ref. [55].

Please cite this article in press as: X.-F. Lin, et al., Graphene-based materials for polymer solar cells, Chin. Chem. Lett. (2016), http://dx.doi.org/10.1016/j.cclet.2016.06.041

Table 1
Summary of graphene and graphene-based composites used in PSCs.

Materials	Function	R_S (kΩ/square)	Device structures	PCE (%)	Reference
rGO	Transparent electrode	3.2	PET substrate/rGO/PEDOT:PSS/P3HT:PCBM/TiO_2/Al	0.78	[32]
rGO	Transparent electrode	17.9	rGO/PEDOT:PSS/P3HT:PCBM/LiF/Al	0.13	[33]
GME	Transparent electrode	0.608	SiO_2/GME/PEDOT:PSS/P3HT:PCBM/LiF/Al	2.04	[34]
MLG	Transparent electrode	0.374	MLG/PEDOT:PSS/P3HT:PCBM/Ca/Al	1.17	[35]
Single-layer Graphene	Transparent electrode	0.105	Graphene/PEDOT:PSS/P3HT:PCBM/ZnO/ITO	2.7	[36]
Graphene	Transparent electrode	0.158	Graphene/PEDOT:PSS/P3HT:PCBM/ZnO/Ag/PI	3.2	[37]
Graphene	Transparent electrode	0.32	Graphene/PEDOT:PSS/PTB7:PC_{71}BM/ZnO-NP/PEDOT:PSS/Graphene/Glass	~3.4	[38]
Au-doped single layer graphene nanoribbons (SLGNRs)	Transparent electrode	0.22	Glass/SLGNRs/PEDOT:PSS/WO3/SMPV1:PC_{71}BM/ZnO/PEDOT:PSS/PTTBDT-FTT:PC_{71}BM/Ca/Al	8.48	[39]
ZnO@graphene core–shell type quantum dots (ZGQDs)	EEL		ITO/PEIE/ZGQD-OAs/PTB7:PC_{71}BM/MoO_3/Ag	10.3	[45]
Metal chloride-doped GO	HEL		ITO/metal chloride-doped GO/PTB7:PC_{71}BM/Ca/Al	6.58	[46]
r-GO functionalized with a sulfonic acid group (sr-GO)	HEL		ITO/sr-GO/PTB7:PC_{71}BM/Ca/Al	7.18	[47]
ZnO@graphene:ethyl cellulose (ZnO@G:EC)	EEL		ITO/ZnO@G:EC/PTB7:PC_{71}BM/MoO_3/Ag	8.4	[48]
layer-by-layer GO (LBL-GO)	HEL		ITO/LBL-GO/P3HT:ICBA/Ca/Al	6.04	[49]
PEGylated Au NP/GO composites (Au@PEG–GO)	HEL and active layer additive		ITO/PEDOT:PSS(Au@PEG–GO)/PBDTTT-CT:PC_{71}BM(Au@PEG–GO)/Ca/Al	7.26	[50]
GO	HEL		ITO/GO/P3HT:PCBM/Al	3.5	[51]
GO	HEL		ITO/GO-PEDOT:PSS/P3HT:PCBM/Al	3.98	[53]
GO-OSO_3H	HEL		ITO/GO-OSO_3H/P3HT:PCBM/Ca/Al	4.37	[54]
Cl-GO	HEL		ITO/Cl-GO/PBDTTT-C:PC_{71}BM/Ca/Al	7.6	[55]
GO/GO-Cs	HEL/EEL		ITO/GO/P3HT:PCBM/GO-Cs/Al	3.67	[57]
GQDs	EEL additive		ITO/GQDs:Cs_2CO_3/P3HT:PCBM/V_2O_5/Au	3.17	[58]
GQDs-Cs_2CO_3	EEL		ITO/GQDs-Cs_2CO_3/P3HT:PCBM/V_2O_5/Au	3.23	[59]
F-GQDs	EEL		ITO/F-GQDs/PTB7:PC_{71}BM/LiF/Al	7.91	[60]
GQDs-TMA	EEL		ITO/PEDOT:PSS/PTB7-Th:PC_{71}BM/GQDs-TMA/Al	8.80	[61]
rGO/$CuInS_2$ quantum dots (rGO/$CuInS_2$-QDs)	Acceptor		ITO/TiO_2/MEH-PPV:rGO/$CuInS_2$-QDs/PEDOT:PSS/Au	1.48	[63]
laser GO-ethylene-dinitro-benzoyl (LGO-EDNB)	Acceptor		ITO/PEDOT:PSS/PCDTBT:LGO-EDNB/TiO_x/Al	2.41	[64]
SPFGraphene	Acceptor		ITO/PEDOT:PSS/P3OT:SPFGraphene/LiF/Al	1.4	[65]
SPFGraphene	Acceptor		ITO/PEDOT:PSS/P3HT:SPFGraphene/LiF/Al	1.1	[66]
G-P3HT	Donor		ITO/PEDOT:PSS/G-P3HT:C_{60}/Al	0.61	[67]
C_{60}-G:P3HT	Acceptor		ITO/PEDOT:PSS/C_{60}-G:P3HT/Al	1.22	[68]
GQDs	Acceptor		ITO/PEDOT:PSS/P3HT:GQDs/Al	1.28	[70]
Aniline functionalized GQDs (ANI-GQDs)	Acceptor		ITO/PEDOT:PSS/P3HT:ANI-GQDs/Al	1.14	[71]
GQDs	Active layer additive		ITO/PEDOT:PSS/P3HT:PCBM:GQDsLiF/Al	5.24	[72]
GOQDs	Active layer additive		ITO/PEDOT:PSS/GOQDs:PTB7:PC_{71}BM/Al	7.6	[73]
N-doped Graphene	Active layer additive		ITO/PEDOT:PSS/N-doped Graphene:P3HT:PCBM/Al	4.5	[74]

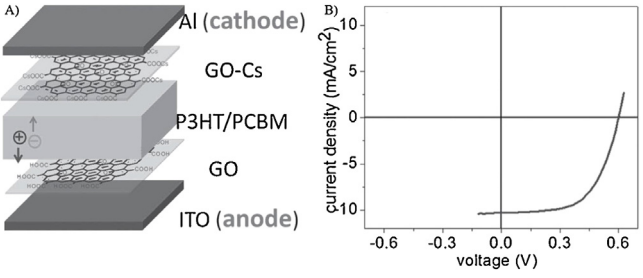

Fig. 11. (A) Device structures of the normal device with GO as hole-extraction layer and GO-Cs as the electron-extraction layer. (B) *J–V* curve of the normal device with both GO and GO-Cs. Reproduced with permission from Ref. [57].

attributed to better electron-extraction, lower work function (shift from 4.55 eV of ITO to 4.18 eV) and the inhibition of charge recombination by GQDs. Liu *et al.* developed two kinds of novel GQDs to fabricate highly efficient PSCs, which were few-layered GQDs (F-GQDs) as HELs [60] and tetramethylammonium functionalized GQDs (GQDs-TMA) as EELs [61]. Owing to its high work function, good film-forming property and high transmittance, F-GQDs-based devices showed a PCE of up to 7.91%, much higher than those of the devices using GO and PEDOT:PSS. On the other hand, GQDs-TMA as EELs can form an interfacial dipole with the metal cathode and thus result in the decrease of the work function from 4.3 eV (Al), 4.7 eV (Ag) and 5.1 eV (Au) to 3.3 eV, 3.6 eV and 3.7 eV, respectively. For the PSCs using poly [4,8-bis[(2-ethylhexylthienyl-5-)benzo[1,2-b:4,5-b0]dithiophene-2,6-diyl][3-uoro-2-[(2-ethylhexyl)carbonyl]thieno[3,4-b]thiophenediyl]](PTB7-Th):PC_{71}BM as active layers and GQDs-TMA as EELs, an optimized PCE of 8.80% is achieved, which is comparable to that of the devices with the normal EELs (*e.g.* Ca, LiF and ZnO). These results indicate that solution-processed GQDs could be prospective interfacial materials for PSCs.

Obviously, the intrinsic characteristics of graphene-based materials can be tuned to meet the special requirement as the interfacial layers by either controlled chemical modification or physical treatment for highly-efficient PSCs. So far, graphene-based materials have shown great potential to replace the most used PEDOT:PSS as HELs, which relies on the fact that they can be deposited from neutral aqueous suspensions and render efficiency values comparable, even superior to the conventional device containing PEDOT:PSS as HELs together with better long-term stability of the device. Further optimization of the structure and fabrication process of graphene-based HELs in PSCs should lead to great improvements in overall device performance. On the other

Please cite this article in press as: X.-F. Lin, et al., Graphene-based materials for polymer solar cells, Chin. Chem. Lett. (2016), http://dx.doi.org/10.1016/j.cclet.2016.06.041

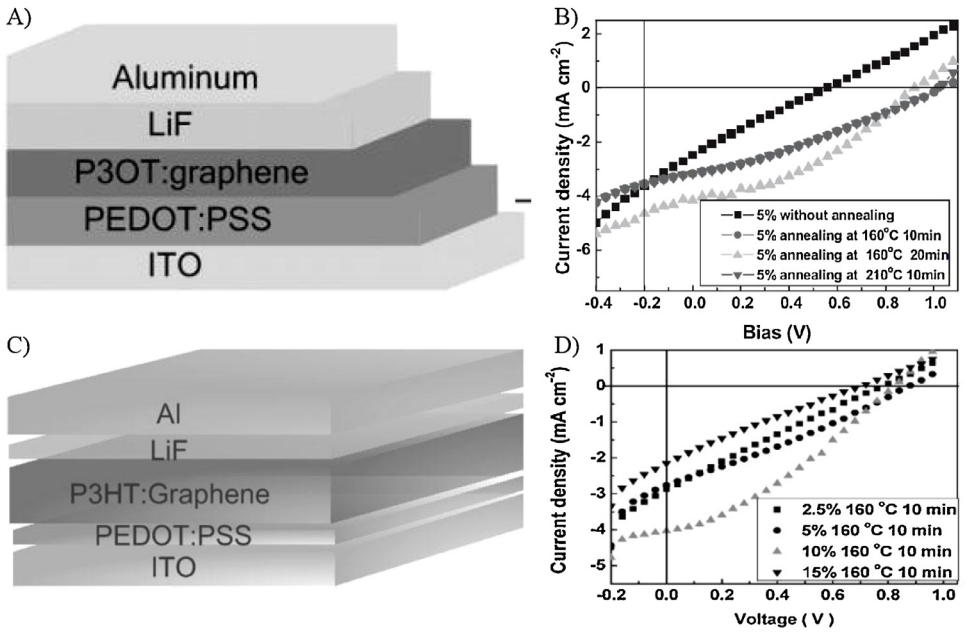

Fig. 12. (A) Schematic of the device with P3OT/graphene thin film as the active layer. (B) *J–V* curves of PSCs based on P3OT/SPFGraphene composite with SPFGraphene content of 5 wt% without annealing, after annealing at 160 °C for 10 min and 20 min, and at 210 °C for 10 min. (C) The schematic structure of P3HT/SPFGraphene. (D) *J–V* curves of the P3HT/SPFGraphene-based PSCs with different graphene contents and different annealing time. The highest PCE is achieved at 10 wt%, 160 °C, 10 min. (A) and (B) Reproduced with permission from Ref. [65]. (C) and (D) Reproduced with permission from Ref. [66].

hand, the chemical reduction of GO can induce the transition of GO from an electrical insulator to a semiconductor. Thus, one main research trend is to develop effective strategies to obtain functionalized GO with tunable work function and electronic properties using desirable reagents for diverse demanding applications. As for EELs materials, it is highly required to achieve low work function, highly conductive materials to improve electron mobility, which can realized by controlled chemical doping of graphene.

4. Graphene-based materials as active layers

The development of acceptor materials in PSCs mainly focused on fullerene and its soluble derivatives, such as PCBM ($PC_{71}BM$), which was one of the most widely used materials as acceptors. However, the fullerene materials are limited by low-efficient hopping charge transport of their spherical structures, leading to the obstruction of charge transport, and high-cost undesirable for large-scale fabrication [62]. As an allotrope of fullerenes, graphene has been regarded as a good candidate to replace fullerenes and its derivatives as excellent acceptor materials owing to its high carrier mobility and unique two-dimensional structure, beneficial for the collection and transport of charge carriers [63,64]. Furthermore, theoretical studies have predicted that the PCE of single junction and tandem PSCs using graphene-based materials as acceptors could even achieve 12% and 24%, respectively [24]. Chen *et al.* [65] demonstrated the first use of graphene derivative as an acceptor and poly(3-octylthiophene) (P3OT) as a donor in PSCs (as shown in Fig. 12A). The best PCE of the devices, optimized by tuning the content of incorporated graphene in active layers (5 wt%) and annealing process (20 min at 160 °C), reached 1.4% (as shown in Fig. 12B). In addition, Chen *et al.* [66] also used such functionalized graphene (the optimal content of 10 wt%) as an acceptor to blend with another typical donor (P3HT) in PSCs, which yields a PCE of 1.1% (Fig. 12C and D). Although the remarkable result by Chen can be comparable with the best PSCs using non-fullerene materials as acceptors, there is still plenty of room for further improvement in device performance.

Recently, Yu *et al.* [67] have chemically grafted CH_2OH-terminated P3HT onto the surface of GO with the carboxylic group (as shown in Fig. 13) by the esterification reaction. The resultant P3HT-grafted GO sheets (G-P3HT) could be soluble in a range of organic solvents after chemical grafting, suitable for solution processing. Photoluminescence results showed that G-P3HT can facilitate exciton dissociation and charge transfer, advantageous for use in solar cells. They used G-P3HT/C_{60} as active layer to build a bilayer photovoltaic device, showing a PCE of 0.61% with 200% enhancement relative to the device based on P3HT/C_{60}. The chemical grafting of P3HT onto graphene can enhance electron delocalization and light absorption, thus resulting in the PCE enhancement.

Following their earlier effort [67], Yu *et al.* [68] chemically grafted C_{60} onto the surface of rGO nanosheets *via* a simple lithiation reaction, and they used the resultant C_{60}-grafted graphene nanosheets as electron acceptors in active layer to fabricate bulk heterojunction solar cells (the device structure as shown in Fig. 14A). Compared to a cell with only C_{60} as an acceptor (0.47%), a 2.5-fold increase of PCE (1.22%, Fig. 14B, Table 1) was obtained for the device using the graphene–C_{60} hybrid material as an electron acceptor, which is higher than many high-performance PSCs with non-fullerene electron acceptors, such as functionalized

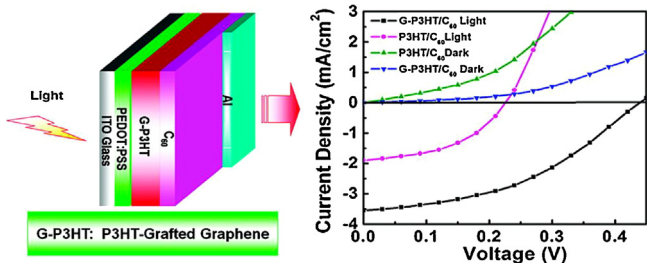

Fig. 13. Schematic of a ITO/PEDOT:PSS/G-P3HT:C_{60}/Al PSC and the *J–V* characteristics of the PSCs using P3HT:C_{60} or G-P3HT:C_{60} as the active layer. Reproduced with permission from Ref. [67].

Please cite this article in press as: X.-F. Lin, et al., Graphene-based materials for polymer solar cells, Chin. Chem. Lett. (2016), http://dx.doi.org/10.1016/j.cclet.2016.06.041

graphene (1.1%) [66] and C_{60}-multiwalled carbon nanotube complex (0.80%) [69]. Such enhancement in the PCE of the devices with the graphene–C_{60} hybrid acceptor is mainly due to the improvement of the electron transport properties, since the incorporation of the graphene–C_{60} hybrid into the active layer of the device could lead to the formation of more efficient electron transport pathway through percolation of the highly conducting two-dimensional graphene sheets.

Owing to the intrinsic characteristics of zero defect, graphene is one of zero-gap semiconductor materials. In order to fully exploit the use of graphene-based materials in PSCs, it is very necessary to introduce band gap into the graphene [70]. Converting the 2D graphene into 0D GQDs is one of the most effective methods to open the band gap of graphene. Li *et al.* [70] demonstrated the first preparation of GQDs with sizes of 3–5 nm by using an electrochemical approach. They found that GQDs can be used as good electron-acceptors for the PSCs. In these devices with the structure of ITO/PEDOT:PSS/P3HT:GQDs/Al (Fig. 15), the LUMO level of the GQDs was tested to be in the range of 4.2–4.4 eV and the HOMO level for P3HT was 5.2 eV, thus leading to a V_{oc} of 0.8 eV, which is higher than the V_{oc} of P3HT:PCBM-based PSCs (0.6 V). The GQDs-based devices produce a PCE of 1.28%. In the meantime, Gupta *et al.* [71] prepared aniline modified GQDs by hydrothermal approach and consequently used them as acceptors in the PSCs with the donor of P3HT (as shown in Fig. 15C). Compared with the best devices used graphene sheets as acceptors (0.65%), the optimized PCE of the GQDs-based devices can reach 1.14% (Fig. 15C).

Followed by the above work, Li *et al.* [72] have fabricated GQDs derived from double-walled carbon nanotubes and blended them into the active layer to align the band structures between the donor and acceptor (Fig. 16A). The GQDs with a uniform size distribution were prepared *via* solution-based method, which can emit blue emission under UV excitation in chlorobenzene. After incorporating the GQDs into the active layer of P3HT:PCBM-based PSCs, a considerable increase of PCE was achieved compared with the conventional device without GQDs, producing a PCE of 5.24%. Kim *et al.* [73] utilized reduction-controlled GQDs (GOQDs), which were blended with efficient active layer of polymer thieno[3,4-b]thiophene/benzodithiophene (PTB7):$PC_{71}BM$, to increase the optical absorptivity and charge carrier extraction of PSCs (Fig. 16C). The GOQDs-based devices showed significant enhancement of the optical absorptivity, leading to the increase of J_{sc} because of the rich functional groups on the surface of GOQDs. In spite of this fact, owing to the metallic property of the GOQDs, charge carrier extraction in the PSCs was increased as well, leading to the improvement of the FF. After balancing optical absorptivity and electrical conductivity of the GOQDs, the optimized PCE of devices was increased from 6.7% to 7.6% relative to the reference devices without GOQDs.

Alternatively, doping graphene with heteroatom is another viable method to modulate its band gap. Jun *et al.* [74] obtained an improved PCE in P3HT:PCBM-based solar cells *via* blending nitrogen-doped (N-doped) graphene flakes with the active layers (Fig. 17). The charge-selective graphene flakes can provide transport pathways for specific charge carriers to transport, when incorporated into the active layer of PSCs. The best PCE (4.5%) of the fabricated PSCs based on N-doped graphene has increased by 40% relative to the reference devices without graphene (3.2%).

Although the aforementioned work has partly addressed some issues of graphene-based materials used in the active layers of PSCs, including the dispersion in the organic solvent [65–68], the optimization of electron transport between donors and acceptors [72] and improvement of the optical utilization in active layer [73]. However, the overall performance of those devices using

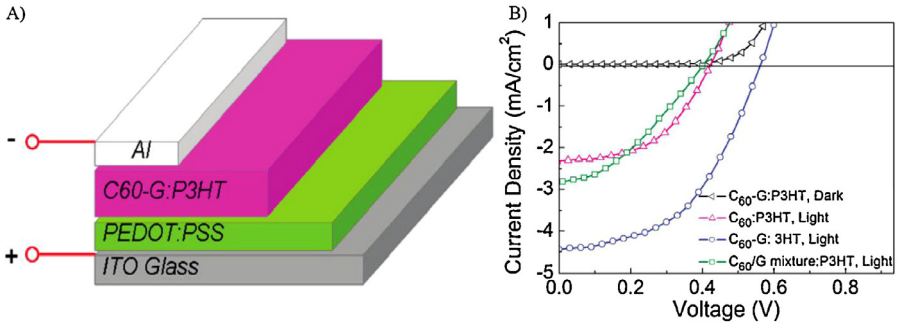

Fig. 14. (A) Schematic of a PSC with the C_{60}-G:P3HT composite as the active layer. (B) *J–V* curves of the PSCs with the C_{60}-G:P3HT (1:1 wt/wt), the C_{60}:P3HT (1:1 wt/wt), or the C_{60}/G mixture (12 wt%):P3HT (1:1 wt/wt) as the active layers after annealing treatment (130 °C, 10 min). Reproduced with permission from Ref. [68].

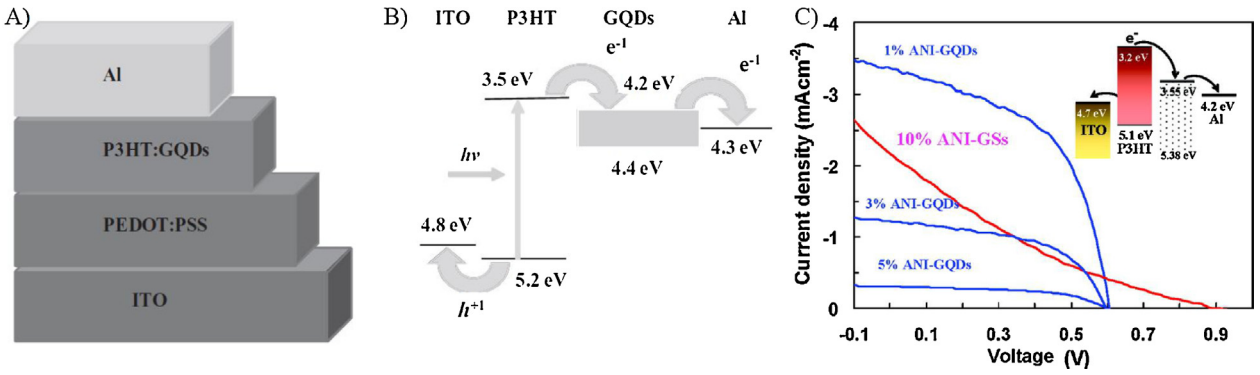

Fig. 15. Schematic (A) and energy band (B) diagrams of the PSCs (ITO/PEDOT:PSS/P3HT:GQDs/Al). (C) *J–V* curves of the PSCs based on ANI-GQDs with different GQDs content. (A) and (B) Reproduced with permission from Ref. [70]. (C) Reproduced with permission from Ref. [71].

Please cite this article in press as: X.-F. Lin, et al., Graphene-based materials for polymer solar cells, Chin. Chem. Lett. (2016), http://dx.doi.org/10.1016/j.cclet.2016.06.041

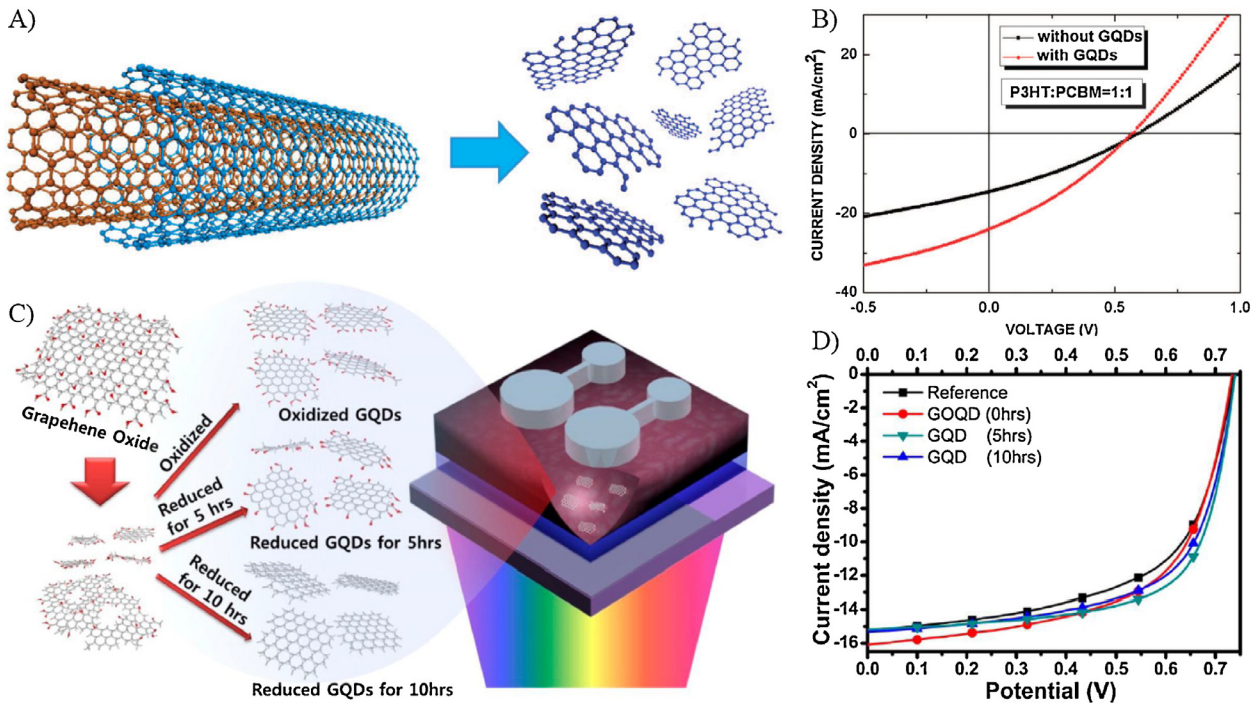

Fig. 16. (A) Schematic showing the preparation of the GQDs. (B) *J–V* curves of the PSCs based on P3HT:PCBM (weight ratio 1:1) blended films with and without GQDs. (C) Schematic of a PSC with three different types of GOQDs, of which edge functional groups are tuned by thermal reduction time. (D) *J–V* curves of the reference and three different GOQD-PSCs. (A) and (B) Reproduced with permission from Ref. [72]. (C) and (D) Reproduced with permission from Ref. [73].

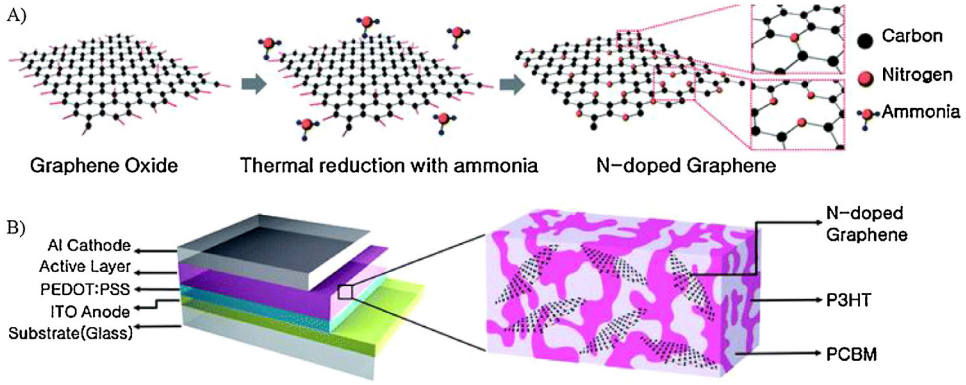

Fig. 17. (A) Schematic of the nitrogen doping process of rGO and (B) the PSCs using the N-doped graphene/P3HT:PCBM active layer fabricated in this work. Reproduced with permission from Ref. [74].

graphene-based materials in active layer is still poorer than that of conventional PSCs using C_{60} and its derivatives and graphene-based materials cannot be used as effective electron acceptors to replace C_{60} derivatives for highly efficient PSCs. Further studies should be undertaken on PSCs with graphene-based electron acceptors, which include: (1) controlling the grain size and layer structure of the graphene acceptor; (2) matching the band structures between the donor–acceptor pairs; and (3) optimization of the device fabrication processes.

5. Conclusion and outlook

In this review, the recent progress of graphene-based materials used in PSCs has been summarized. Due to its unique properties and versatility, graphene has emerged as a type of material useful in a range of device parts including the transparent electrode, active layer, and interfacial layer. The huge potential of graphene has been widely demonstrated in low-cost and efficient solar cells with additional advantages suitable for flexible/wearable devices. Although graphene-based materials have shown many distinctive advantages and great potential to replace some traditional materials (*e.g.* ITO, PEDOT:PSS) used in various layers of PSCs, there still exists a large number of additional challenges for the use of graphene as a key component in PSCs. Firstly, new preparation methods should be developed to produce continuous, large-area, high quality graphene thin film with controlled morphology and electronic properties, since the performance of graphene-based PSCs is closely associated with the intrinsic properties of graphene including its purity, band-gap, structural uniformity. Particularly for graphene transparent electrodes, it is highly desirable to seek new solution-based strategies to achieve large-area graphene thin film with a good balance of high transparency and low sheet

Please cite this article in press as: X.-F. Lin, et al., Graphene-based materials for polymer solar cells, Chin. Chem. Lett. (2016), http://dx.doi.org/10.1016/j.cclet.2016.06.041

resistance, since the main challenge of using graphene in polymer as transparent electrodes is the preparation of large-area devices by a solution process. Secondly, new doping or functionalization techniques compatible with the fabrication process of solar cells should be exploited to realize high charge carrier densities, excellent stability and tunable energy levels in graphene. Thirdly, developing new types of graphene materials such as GQDs are another important research trend. Due to quantum confinement and edge effect, the GQDs could exhibit some unique properties, which could allow for the fabrication of all graphene-based solar cells. Therefore, it is highly anticipated that continuous innovative efforts toward the development of graphene-based materials and device fabrication techniques for high performance PSCs could bring a new future prospect for the solar energy industry.

Acknowledgments

The authors are grateful to the Natural Science Foundations of China (Nos. 51573214, 51233008) and the Youth 1000 Talent Program of China.

References

[1] G. Yu, J. Gao, J.C. Hummelen, F. Wudl, A.J. Heeger, Polymer photovoltaic cells: enhanced efficiencies via a network of internal donor–acceptor heterojunctions, Science 270 (1995) 1789–1791.
[2] J.Y. Kim, K. Lee, N.E. Coates, et al., Efficient tandem polymer solar cells fabricated by all-solution processing, Science 317 (2007) 222–225.
[3] G. Li, R. Zhu, Y. Yang, Polymer solar cells, Nat. Photon. 6 (2012) 153–161.
[4] J. Liu, M. Durstock, L.M. Dai, Graphene oxide derivatives as hole-and electron-extraction layers for high-performance polymer solar cells, Energy Environ. Sci. 7 (2014) 1297–1306.
[5] M.T. Dang, L. Hirsch, G. Wantz, J.D. Wuest, Controlling the morphology and performance of bulk heterojunctions in solar cells. Lessons learned from the benchmark poly(3-hexylthiophene):[6,6]-phenyl-C61-butyric acid methyl ester system, Chem. Rev. 113 (2013) 3734–3765.
[6] Y.H. Liu, J.B. Zhao, Z.K. Li, et al., Aggregation and morphology control enables multiple cases of high-efficiency polymer solar cells, Nat. Commun. 5 (2014) 5293.
[7] B. Yang, Y.B. Yuan, P. Sharma, et al., Tuning the energy level offset between donor and acceptor with ferroelectric dipole layers for increased efficiency in bilayer organic photovoltaic cells, Adv. Mater. 24 (2012) 1455–1460.
[8] X.P. Xu, Z.J. Li, Z.G. Wang, et al., 10.20% efficiency polymer solar cells via employing bilaterally hole-cascade diazaphenanthrobisthiadiazole polymer donors and electron-cascade indene-C70 bisadduct acceptor, Nano Energy 25 (2016) 170–183.
[9] K. Li, Z.J. Li, K. Feng, et al., Development of large band-gap conjugated copolymers for efficient regular single and tandem organic solar cells, J. Am. Chem. Soc. 135 (2013) 13549–13557.
[10] S.K. Hau, H.L. Yip, A.K.Y. Jen, A review on the development of the inverted polymer solar cell architecture, Polym. Rev. 50 (2010) 474–510.
[11] Z.C. He, C.M. Zhong, S.J. Su, et al., Enhanced power-conversion efficiency in polymer solar cells using an inverted device structure, Nat. Photon. 6 (2012) 593–597.
[12] J.B. You, C.C. Chen, L.T. Dou, et al., Metal oxide nanoparticles as an electron-transport layer in high-performance and stable inverted polymer solar cells, Adv. Mater. 24 (2012) 5267–5272.
[13] X.F. Lin, Y.Z. Yang, L. Nian, et al., Interfacial modification layers based on carbon dots for efficient inverted polymer solar cells exceeding 10% power conversion efficiency, Nano Energy 26 (2016) 216–223.
[14] J.B. You, L.T. Dou, K. Yoshimura, et al., A polymer tandem solar cell with 10.6% power conversion efficiency, Nat. Commun. 4 (2013) 1446–1455.
[15] A.K. Geim, K.S. Novoselov, The rise of graphene, Nat. Mater. 6 (2007) 183–191.
[16] D. Chen, H. Zhang, Y. Liu, J.H. Li, Graphene and its derivatives for the development of solar cells, photoelectrochemical, and photocatalytic applications, Energy Environ. Sci. 6 (2013) 1362–1387.
[17] D.W. Chang, H.J. Choi, A. Filer, J.B. Baek, Graphene in photovoltaic applications: organic photovoltaic cells (OPVs) and dye-sensitized solar cells (DSSCs), J. Mater. Chem. A 2 (2014) 12136–12149.
[18] Z.K. Liu, S.P. Lau, F. Yan, Functionalized graphene and other two-dimensional materials for photovoltaic devices: device design and processing, Chem. Soc. Rev. 44 (2015) 5638–5679.
[19] L.T. Qu, Y. Liu, J.B. Baek, L.M. Dai, Nitrogen-doped graphene as efficient metal-free electrocatalyst for oxygen reduction in fuel cells, ACS Nano 4 (2010) 1321–1326.
[20] J.Y. Luo, W.J. Cui, P. He, Y.Y. Xia, Raising the cycling stability of aqueous lithium-ion batteries by eliminating oxygen in the electrolyte, Nat. Chem. 2 (2010) 760–765.
[21] L.M. Dai, Functionalization of graphene for efficient energy conversion and storage, Acc. Chem. Res. 46 (2013) 31–42.
[22] D.S. Yu, K.L. Goh, H. Wang, et al., Scalable synthesis of hierarchically structured carbon nanotube-graphene fibres for capacitive energy storage, Nat. Nanotechnol. 9 (2014) 555–562.
[23] D.S. Yu, Q. Qian, L. Wei, et al., Emergence of fiber supercapacitors, Chem. Soc. Rev. 44 (2015) 647–662.
[24] V. Yong, J.M. Tour, Theoretical efficiency of nanostructured graphene-based photovoltaics, Small 6 (2010) 313–318.
[25] J. Kim, V.C. Tung, J.X. Huang, Water processable graphene oxide: single walled carbon nanotube composite as anode modifier for polymer solar cells, Adv. Energy Mater. 1 (2011) 1052–1057.
[26] I.P. Murray, S.J. Lou, L.J. Cote, et al., Graphene oxide interlayers for robust, high-efficiency organic photovoltaics, J. Phys. Chem. Lett. 2 (2011) 3006–3012.
[27] D.H. Wang, J.K. Kim, J.H. Seo, et al., Transferable graphene oxide by stamping nanotechnology: electron-transport layer for efficient bulk-heterojunction solar cells, Angew. Chem. Int. Ed. 52 (2013) 2874–2880.
[28] J.C. Yu, J.I. Jang, B.R. Lee, et al., Highly efficient polymer-based optoelectronic devices using PEDOT:PSS and a GO composite layer as a hole transport layer, ACS Appl. Mater. Interfaces 6 (2014) 2067–2073.
[29] A.R.B.M. Yusoff, S.J. Lee, F.K. Shneider, W.J. da Silva, J. Jang, High-performance semitransparent tandem solar cell of 8.02% conversion efficiency with solution-processed graphene mesh and laminated Ag nanowire top electrodes, Adv. Energy Mater. 4 (2014) 3412–3420.
[30] Y.H. Chen, W.C. Lin, J. Liu, L.M. Dai, Graphene oxide-based carbon interconnecting layer for polymer tandem solar cells, Nano Lett. 14 (2014) 1467–1471.
[31] J.H. Du, S.F. Pei, L.P. Ma, H.M. Cheng, 25th anniversary article: carbon nanotube-and graphene-based transparent conductive films for optoelectronic devices, Adv. Mater. 26 (2014) 1958–1991.
[32] Z.Y. Yin, S.Y. Sun, T. Salim, et al., Organic photovoltaic devices using highly flexible reduced graphene oxide films as transparent electrodes, ACS Nano 4 (2010) 5263–5268.
[33] Y.F. Xu, G.K. Long, L. Huang, et al., Polymer photovoltaic devices with transparent graphene electrodes produced by spin-casting, Carbon 48 (2010) 3308–3311.
[34] Q. Zhang, X.J. Wan, F. Xing, et al., Solution-processable graphene mesh transparent electrodes for organic solar cells, Nano Res. 6 (2013) 478–484.
[35] Y.Y. Choi, S.J. Kang, H.K. Kim, W.M. Choi, S.I. Na, Multilayer graphene films as transparent electrodes for organic photovoltaic devices, Sol. Energy Mater. Sol. Cells 96 (2012) 281–285.
[36] Z.K. Liu, J.H. Li, Z.H. Sun, et al., The application of highly doped single-layer graphene as the top electrodes of semitransparent organic solar cells, ACS Nano 6 (2012) 810–818.
[37] Z.K. Liu, J.H. Li, F. Yan, Package-free flexible organic solar cells with graphene top electrodes, Adv. Mater. 25 (2013) 4296–4301.
[38] Z.K. Liu, P. You, S.H. Liu, F. Yan, Neutral-color semitransparent organic solar cells with all-graphene electrodes, ACS Nano 9 (2015) 12026–12034.
[39] A.R.b.M. Yusoff, D. Kim, F.K. Schneider, et al., Au-doped single layer graphene nanoribbons for a record-high efficiency ITO-Free tandem polymer solar cells, Energy Environ. Sci. 8 (2015) 1523–1537.
[40] H. Ma, H.L. Yip, F. Huang, A.K.Y. Jen, Interface engineering for organic electronics, Adv. Funct. Mater. 20 (2010) 1371–1388.
[41] M. Girtan, M. Rusu, Role of ITO and PEDOT:PSS in stability/degradation of polymer: fullerene bulk heterojunctions solar cells, Sol. Energy Mater. Sol. Cells 94 (2010) 446–450.
[42] M. Jørgensen, K. Norrman, F.C. Krebs, Stability/degradation of polymer solar cells, Sol. Energy Mater. Sol. Cells 92 (2008) 686–714.
[43] W.J.E. Beek, M.M. Wienk, M. Kemerink, X.N. Yang, R.A.J. Janssen, Hybrid zinc oxide conjugated polymer bulk heterojunction solar cells, J. Phys. Chem. B. 109 (2005) 9505–9516.
[44] A.K.K. Kyaw, D.H. Wang, V. Gupta, et al., Efficient solution-processed small-molecule solar cells with inverted structure, Adv. Mater. 25 (2013) 2397–2402.
[45] B.J. Moon, K.S. Lee, J. Shim, et al., Enhanced photovoltaic performance of inverted polymer solar cells utilizing versatile chemically functionalized ZnO@graphene quantum dot monolayer, Nano Energy 20 (2016) 221–232.
[46] E.S. Choi, Y.J. Jeon, S.S. Kim, et al., Metal chloride-treated graphene oxide to produce high-performance polymer solar cells, Appl. Phys. Lett. 107 (2015) 023301.
[47] J.S. Yeo, J.M. Yun, Y.S. Jung, et al., Sulfonic acid-functionalized, reduced graphene oxide as an advanced interfacial material leading to donor polymer-independent high-performance polymer solar cells, J. Mater. Chem. A 2 (2014) 292–298.
[48] A.F. Hu, Q.X. Wang, L. Chen, et al., In situ formation of ZnO in graphene: a facile way to produce a smooth and highly conductive electron transport layer for polymer solar cells, ACS Appl. Mater. Interfaces 7 (2015) 16078–16085.
[49] L.Y. Zhou, D. Yang, W. Yu, J. Zhang, C. Li, An efficient polymer solar cell using graphene oxide interface assembled via layer-by-layer deposition, Org. Electron. 23 (2015) 110–115.
[50] M.K. Chuang, F.C. Chen, Synergistic plasmonic effects of metal nanoparticle-decorated PEGylated graphene oxides in polymer solar cells, ACS Appl. Mater. Interfaces 7 (2015) 7397–7405.
[51] S.S. Li, K.H. Tu, C.C. Lin, C.W. Chen, M. Chhowalla, Solution-processable graphene oxide as an efficient hole transport layer in polymer solar cells, ACS Nano 4 (2010) 3169–3174.
[52] S. Mao, H.H. Pu, J.H. Chen, Graphene oxide and its reduction: modeling and experimental progress, RSC Adv. 2 (2012) 2643–2662.
[53] Y.J. Jeon, J.M. Yun, D.Y. Kim, S.I. Na, S.S. Kim, High-performance polymer solar cells with moderately reduced graphene oxide as an efficient hole transporting layer, Sol. Energy Mater. Sol. Cells 105 (2012) 96–102.

Please cite this article in press as: X.-F. Lin, et al., Graphene-based materials for polymer solar cells, Chin. Chem. Lett. (2016), http://dx.doi.org/10.1016/j.cclet.2016.06.041

[54] J. Liu, Y.H. Xue, L.M. Dai, Sulfated graphene oxide as a hole-extraction layer in high-performance polymer solar cells, J. Phys. Chem. Lett. 3 (2012) 1928–1933.
[55] D. Yang, L.Y. Zhou, W. Yu, J. Zhang, C. Li, Work-function-tunable chlorinated graphene oxide as an anode interface layer in high-efficiency polymer solar cells, Adv. Energy Mater. 4 (2014) 1400591.
[56] S. Wang, P.K. Ang, Z.Q. Wang, et al., High mobility, printable, and solution-processed graphene electronics, Nano Lett. 10 (2010) 92–98.
[57] J. Liu, Y.H. Xue, Y.X. Gao, et al., Hole and electron extraction layers based on graphene oxide derivatives for high-performance bulk heterojunction solar cells, Adv. Mater. 24 (2012) 2228–2233.
[58] H.B. Yang, Y.Q. Dong, X.Z. Wang, et al., Graphene quantum dots-incorporated cathode buffer for improvement of inverted polymer solar cells, Sol. Energy Mater. Sol. Cells 117 (2013) 214–218.
[59] H.B. Yang, Y.Q. Dong, X.Z. Wang, et al., Cesium carbonate functionalized graphene quantum dots as stable electron-selective layer for improvement of inverted polymer solar cells, ACS Appl. Mater. Interfaces 6 (2014) 1092–1099.
[60] Z.C. Ding, Z. Hao, B. Meng, et al., Few-layered graphene quantum dots as efficient hole-extraction layer for high-performance polymer solar cells, Nano Energy 15 (2015) 186–192.
[61] Z.C. Ding, Z.S. Miao, Z.Y. Xie, J. Liu, Functionalized graphene quantum dots as a novel cathode interlayer of polymer solar cells, J. Mater. Chem. A 4 (2016) 2413–2418.
[62] W.U. Huynh, J.J. Dittmer, A.P. Alivisatos, Hybrid nanorod-polymer solar cells, Science 295 (2002) 2425–2427.
[63] W.L. Meng, X. Zhou, Z.L. Qiu, et al., Reduced graphene oxide-supported aggregates of $CuInS_2$ quantum dots as an effective hybrid electron acceptor for polymer-based solar cells, Carbon 96 (2016) 532–540.
[64] M.M. Stylianakis, M. Sygletou, K. Savva, et al., Photochemical synthesis of solution-processable graphene derivatives with tunable bandgaps for organic solar cells, Adv. Opt. Mater. 3 (2015) 658–666.
[65] Z.F. Liu, Q. Liu, Y. Huang, et al., Organic photovoltaic devices based on a novel acceptor material: graphene, Adv. Mater. 20 (2008) 3924–3930.
[66] Q. Liu, Z.F. Liu, X.Y. Zhang, et al., Polymer photovoltaic cells based on solution-processable graphene and P3HT, Adv. Funct. Mater. 19 (2009) 894–904.
[67] D.S. Yu, Y. Yang, M. Durstock, J.B. Baek, L.M. Dai, Soluble P3HT-grafted graphene for efficient bilayer-heterojunction photovoltaic devices, ACS Nano 4 (2010) 5633–5640.
[68] D.S. Yu, K. Park, M. Durstock, L.M. Dai, Fullerene-grafted graphene for efficient bulk heterojunction polymer photovoltaic devices, J. Phys. Chem. Lett. 2 (2011) 1113–1118.
[69] C. Li, Y.H. Chen, S.A. Ntim, S. Mitra, Fullerene-multiwalled carbon nanotube complexes for bulk heterojunction photovoltaic cells, Appl. Phys. Lett. 96 (2010) 143303.
[70] Y. Li, Y. Hu, Y. Zhao, et al., An electrochemical avenue to green-luminescent graphene quantum dots as potential electron-acceptors for photovoltaics, Adv. Mater. 23 (2011) 776–780.
[71] V. Gupta, N. Chaudhary, R. Srivastava, et al., Luminescent graphene quantum dots for organic photovoltaic devices, J. Am. Chem. Soc. 133 (2011) 9960–9963.
[72] F.S. Li, L.J. Kou, W. Chen, C.X. Wu, T.L. Guo, Enhancing the short-circuit current and power conversion efficiency of polymer solar cells with graphene quantum dots derived from double-walled carbon nanotubes, NPG Asia Mater. 5 (2013) e60.
[73] J.K. Kim, M.J. Park, S.J. Kim, et al., Balancing light absorptivity and carrier conductivity of graphene quantum dots for high-efficiency bulk heterojunction solar cells, ACS Nano 7 (2013) 7207–7212.
[74] G.H. Jun, S.H. Jin, B. Lee, et al., Enhanced conduction and charge-selectivity by N-doped graphene flakes in the active layer of bulk-heterojunction organic solar cells, Energy Environ. Sci. 6 (2013) 3000–3006.

Please cite this article in press as: X.-F. Lin, et al., Graphene-based materials for polymer solar cells, Chin. Chem. Lett. (2016), http://dx.doi.org/10.1016/j.cclet.2016.06.041